LPV Land surface temperature and emissivity

José A. Sobrino & Simon Hook*

Global Change Unit, Image Processing Laboratory,

University of Valencia

***NASA Jet Propulsion Laboratory**

LST/LSE

- LST/LSE are important parameters for environmental monitoring and earth system modelling.

- LST has been observed from spaceborne instruments for several decades

  -High spatial resolution sensors (ASTER, Lansat 5 TM, TIRS Landsat 8, upcoming Sentinel2)

  - Low spatial resolution sensors (MODIS, AVHRR, AATSR, SEVIRI, upcoming SLSTR on Sentinel3)

- Validation of LST is of crucial importance for estimating the accuracy of the operational products and understanding the potential and limitations of Satellite observations of LST

WHY LST IS NOT ECV?

Summary of TIR remote sensing applications identified during the FSS project

Solid Earth: 18
Health & Haz.: 17
Security & Surv.: 6
Total: 41

Topic	Subtopic	Application
Land & Solid Earth	Volcanoes	Eruption clouds
		Tropesperic Plumes
		Hot spots and active lava flows
		Post eruptive studies on lava flows
	Fires	Detection of fires
		Estimation of fire risk
		Estimation of burnt area
	Water management	Detection of water stress in crops
		Detection of water stress in forest
		Detection of evapotranspiration in crops
		Detection of evapotranspiration in River Basin
		Detection of evapotranspiration in continents
	Earthquakes	Detection of earthquakes
	Coal mine fires	Detection of coal mine fires
		Delineation of potential coal fires and coal fire risk areas
	Growing Degree-Day	Growing Degree Day estimations
		Growing Degree Day mapping
		Cooling Degree Day Estimations
Health & Hazards	Urban Heat Island	Vegetation maps
		Land cover/Land Use
		Building Information
		Air Quality
	Epidemiology	Mapping Malaria Potential regions
		Arthropod vector ecology and disease distribution
		Mapping Cholera Potential regions
		Mapping Meningitis outbreak
	Industrial risks	Air pollution
		Differentiate between urban and industrial zone
		Oil spill detection
		Plume detection
	Coastal inundations	Prediction of floods
		Monitoring of floods
		Asbestos-cement detection over non-accesible areas
Security & Surveillance		Detection of minefields and landmines
		Border Security
		Object Monitoring and Detection
	Ship/Port monitoring	Piracy/drug smuggling/Ilegal Immigration
		Industrial/power plant monitoring
		Trafficability (off-road soil moisture content)

Requirements table for Solid Earth applications

Application [Source]	EO Level 2/3 Product	Spatial Resolution	Geographical Coverage	Temporal Resolution	Accuracy	Algorithms	TIR Spectral Resolution	Other spectral ranges	Supporting data
Eruption clouds *[Pugnaghi et al; 2006, Corradini et al. 2008]*	Geophysical variables	1-3 km	Large 1000 – 2000 km	3-4 hours		Time series	Two bands (10 – 12 μm)	UV-VIS	Physical models
Tropospheric Plumes *[Pugnaghi et al; 2006, Corradini et al. 2008]*	Geophysical variables	30-100 m	Medium 100 – 500 km	daily		BTD, LUT	Multispectral (≥ 3 bands in 8-12 μm)	UV-VIS	Physical models, DEM
Hot spots and active lava flows *[Wright et al, 2002]*	Geophysical variables	10 - 50 m	Small 60-100 km	daily	Saturation above 60°	Threshold	11μm	4μm -	Deformation maps - DEM
Post eruptive studies on lava flows *[Harris et al., 2003; Oppenheimer, 1998]*	Geophysical variables	10 – 50 m	Small 100 – 200 km	15 days	Saturation above 60°	Threshold	11μm	SWIR-MIR - SAR	DEM
Detection of fires [*CEOS (2003); Zhukov et al. (2006)*]	Geophysical variables (LST)	100 m	Global	15 minutes	Not critical (hot spots are at least 200 K higher than background)	Temperature threshold from a single image	Multispectral (≥ 3 bands in 8-12 μm)	SWIR (1.5-2.5 μm) MIR (3-5 μm)	Atmospheric constituents for atm correction
Estimation of fire risk [*CEOS (2003)*]	Geophysical variables (Vegetation Index)	30 m	Global	Daily - Weekly	2% (usual accuracy of NDVI estimations)	Multitemporal: Vegetation Condition Index (VCI)	-	VNIR (Red,Green, NIR@0.8μm)	-
Estimation of burnt area [*CEOS (2003); Giglio et al. (2009)*]	Geophysical variables (Vegetation Index)	30 m	Global	Daily - Weekly	2% (usual accuracy of NDVI estimations)	Multitemporal: comparison of reflectance or vegetation index with time series	-	VNIR (Red,Green, NIR@0.8μm)	-
Detection of earthquakes – LST [*Tronin (2000); Tramutoli et al. 2005); Saraf & Choudhury (2005)*]	LST	0.5 – 5 km	200km - global	daily	< 1 K	Split-window (SW) method; Temperature and Emissivity Separation (TES) method	Two bands (10 – 12 μm); Multispectral (≥ 3 bands in 8-12 μm)	VNIR (Red, NIR@0.8μm)	atmospheric water vapor content; Atmospheric constituents for atm correction

Requirements table for Solid Earth applications *(cont.)*

Detection of earthquakes - Emissivity [*Tronin (2000); Tramutoli et al. (2005); Saraf & Choudhury (2005)*]	emissivity	0.5 – 5 km	200km - global	Weekly - monthly	< 0.01	Threshold Method; TES	Multispectral (≥ 3 bands in 8-12 μm)	VNIR (Red, NIR@0.8μm)	Atmospheric constituents for atm correction
Detection of coal mine fires [*J. Zhang et al. (2004); C. Kuenzer et al. (2007b); X. Zhang et al. (2004)*]	Geophysical variables (LST)	1 - 100 m	Local to Regional	Daily-Monthly	Not critical (hot spots are 20 K higher than background)	Temperature threshold from a single image	1 broad-band (8-12 μm) Multiespectral (≥ 3 bands in 8-12 μm)	VNIR (Red,Green, NIR@0.8μm) MIR (3-5 μm)	In-situ temperature to select the threshold is recommendable
Delineation of potential coal fires and coal fire risk areas [*Gao et al. (2006); Gao et al. (2009)*]	Land cover	100 m	Local to Regional	Monthly	-	Classification techniques from a single image	Multiespectral (≥ 3 bands in 8-12 μm)	VNIR (Red,Green, NIR@0.8μm) SWIR (1.5-2.5 μm)	-
Detection of water stress in crops [*Sepulcre-Cantó et al. (2006; 2007)*]	Level 3 (clasifications, consider also visible, near infrared and meteorological data)	2 - 7 m	Local	Daily	1 K	Temperature threshold, classifications techniques	Two bands (10-12 μm)	VNIR	Meteorological data (air temperature)
Detection of water stress in forest [*Dvaux-Ros (1995); Duchemin et al. (1999)*]	Land cover	100 m	Local to Regional	Daily-Monthly	1 K	Temperature threshold, classifications techniques	Two bands (10-12 μm)	VNIR	Meteorological data (air temperature)
Detection of evapotranspiration in crops [*Sobrino et al. (2005;2008)*]	Level 3 (clasifications, consider also visible, near infrared and meteorological data)	1 - 10 m	Local	Instantaneous-Daily	1 K	Energy Balance Models	Two bands (10-12 μm)	VNIR	Meteorological data (Air temperature, relative humidity)
Detection of evapotranspiration in River, Basin, [*Sánchez et al. (2007); Jia et al. (2009)*]	Level 3 (clasifications, consider also visible, near infrared and meteorological data)	100 m	Local to Regional	Daily-Monthly	1 K	Energy Balance Models	Two bands (10-12 μm)	VNIR	Meteorological data (Air temperature, relative humidity, precipitation)
Detection of evapotranspiration in continents [*Fisher et al. (2008)*]	Level 3 (clasifications, consider also visible, near infrared and meteorological data)	1 km	Continental-Global	Daily-Monthly	1 K	Energy Balance Models	Two bands (10-12 μm)	VNIR	Meteorological data (Air temperature, relative humidity, precipitation)

Requirements table for Solid Earth applications *(cont.)*

Growing Degree Day estimations [*Vancutsem et al. (2010); Hassan et al. (2007a)*]	Level-3 Land surface temperature; Vegetation Index (NDVI)	1 Km/20m	Local scale	Daily/Sub-daily	1-2 K	Multivariate Statistical correlation	Two bands (10 – 12 μm) for Split-Window; Multiespectral (≥ 3 bands in 8-12 μm) for TES	VNIR for NDVI 0.63 – 0.69 μm 0.76 – 0.90 μm	Weather station network & Land cover Map
Growing Degree Day mapping [*Mikkelsen & Olesen (1984); Blair et al. (2002); Hassan et al. (2007b)*]	Level-3 LST & Land cover maps	1 Km/20m	Regional to local scale	Daily/Sub-daily	1-2 K	Multivariate Statistical correlation & Spatial Analysis using Computational approach	Two bands (10 – 12 μm) for Split-Window; Multiespectral (≥ 3 bands in 8-12 μm) for TES	VNIR for NDVI 0.63 – 0.69 μm 0.76 – 0.90 μm	Weather station network & Land cover Map
Cooling Degree Day Estimations [*Stathopoulou et al. (2006)*]	Level-3 Land surface temperature	1 Km/20m	Local scale	Daily/Sub-daily	1-2 K	Method proposed by Stathopoulou et al (2006)	Two bands (10 – 12 μm) for Split-Window; Multiespectral (≥ 3 bands in 8-12 μm) for TES	VNIR for NDVI 0.63 – 0.69 μm 0.76 – 0.90 μm	Weather station network & Land cover Map

Requirements table for Health & Hazards applications

Application [Source]	EO Level 2/3 Product	Spatial Resolution	Geographical Coverage	Temporal Resolution	Accuracy	Algorithms	TIR Spectral Resolution	Other spectral ranges	Supporting data
UHI - Vegetation maps *[UHI Proj, 2009]*	Maps	10-100 m	Local-Regional	monthly		Multivariate statistical	Two bands (10 – 12 μm)	Multispectral	Land Cover Maps
UHI - Land cover/Land Use *[UHI Proj, 2009]*	Maps	10-100 m	Local-Regional	monthly		Multivariate statistical	Two bands (10 – 12 μm)	Multispectral-SAR	GIS
UHI - Building Information *[UHI Proj, 2009]*	Temperature	1 - 10 m	Local	monthly	1 – 2 K	LST	Two bands (10 – 12 μm)	SAR	City maps
UHI - Air Quality *[UHI Proj, 2009]*	Temperature	20 m – 1km	Local-Regional	Daily-monthly		Statistical		UV-VIS	Atmo models
Air pollution [*Bowman et al. (2006); Barret et al. (2005)*]	Radiance	100 m	Local- Regional	Daily (at noon)	-	Inversion techniques from IR sounding measurements	Hyperspectral (3-15 μm) FTIR spectroscopy	-	-
Differentiate between urban and industrial zone [*Kato & Yamaguchi (2007)*]	Storage heat flux	100 m	Local	Monthly	LST: 1.5 K Emissivity: 0.015	TES for LST/ε and energy balance	Multiespectral (≥ 3 bands in 8-12 μm)	VNIR data for albedo	Meteorological data and surface roughness
Oil spill detection [*Shcherbak et al. (2008); Tseng & Chiu (1994)*]	Temperature	100m-1Km	Local-Regional	Few hours	1 K	Temperature threshold (LST from split-window)	Two bands (10 – 12 μm)	Combination between VNIR and RADAR	
Plume detection [*Chrysoulakis (2002); Chrysoulakis & Cartalis (2003); Chrysoulakis et al. (2005)*]	Temperature CLD	100m-1Km	Local	Few hours	1 K	Classification and temperature threshold (LST from split-window)	Two bands (10 – 12 μm)	VNIR for NDVI 0.63 – 0.69 μm 0.76 – 0.90 μm	
Prediction of floods [*Billa et al. (2006); Feidas et al. (2000); Morales et al. (2003)*]	Level 3 (classifications, consider also visible and near-infrared)	500m - 1km	Regional	Daily	-	Temperature threshold, classifications techniques	Two bands (10-12 μm)	VNIR or Passive microwave	Lighting information from long-range network
Monitoring of floods [*Roshier et al. (2004); Lakshmi et al. (2001)*]	Level 3 (thresholds)	1m - 1 km	Local to Regional	Daily (Noon-Midnight)	1 K	Temperature threshold from a single image	Multiespectral (≥ 3 bands in 8-12 μm)	-	-

Requirements table for Health & Hazards applications *(cont.)*

Mapping Malaria Potential regions [*Green & Hay (2002); Gemperli et al. (2004); Rahman et al. (2006)*]	Level-3 Land surface temperature; Vegetation Index (NDVI)	1 Km/100 m	Continental to Regional scale	Daily/sub-daily	< 2K	Split-window	Two bands (10 – 12 µm)	VNIR for NDVI	Meteorological data
Arthropod vector ecology and disease distribution [*Marj et al. (2008); Gemperli et al. (2004)*]	Level-3 LST & Land cover maps	1 Km /100 m	Continental to Regional scale	10 days composite/sub-daily	< 2K	Split-window	Two bands (10 – 12 µm)	VNIR for NDVI	Meteorological data
Mapping Cholera Potential regions [*Gil et al. (2004); Lobitz et al. (2000); Emch et al. (2008)*]	Level-3 ; SST and Chlorophyll concentrations	1 Km /100m	Continental to Regional scale	Daily/sub-daily	< 1K	Split-window	Two bands (10 – 12 µm)	VNIR (blue and green channels for chlorophyll)	Meteorological data
Mapping Meningitis outbreak [*Gemperli et al. (2004)*]	Level-3 ; LST and Dust Blown map	5 Km /100m	Continental to Regional scale	Daily/sub-daily	< 2K	Split-window	Two bands (10 – 12 µm)	VNIR for NDVI	Meteorological data
Asbestos-cement detection over non-accesible areas [*Bassani et al. (2007)*]	Level-2 (radiance) Level 3 Emissivity at high spatial level	20m/3m	Local scale	Monthly/daily	Not critical, only relative values are used	Temperature and Emissivity Separation algorithms	Hyperspectral (with a band in 9.44 µm)	VNIR for visual inspection recommendable	Laboratory analysis, mineralogical composition, in-situ measurements

Requirements table for Security & Surveillance applications

Application [Source]	EO Level 2/3 Product	Spatial Resolution	Geographical Coverage	Temporal Resolution	Accuracy	Algorithms	TIR Spectral Resolution	Other spectral ranges	Supporting data
Detection of minefields and landmines [Maathuis and van Genderen, 2004]	LST	2 cm – 8 cm (landmines) 1-5 m (minefields)	Local	Overpass time: sunrise, sunset	<0.5ºC	Split-window (SW); Temperature and Emissivity Separation (TES)	Two bands (10 – 12 µm); Multispectral (≥ 3 bands in 8 – 12 µm)	VNIR (Red, NIR@0.8µm)	Emissivity, water vapor content
Border Security [Personal Interview]	2= TOA Brightness Temp	~15m	Europe + N Africa to 5ºN	1-2 days				SAR	DEM
Object Monitoring and Detection [Personal Interview]	2 =TOA Brightness Temp	~10m	Local			Two dimensional MRTD models	1 band: 0.8 - 2.5 µm	SAR	DEM
Ship & port monitoring: Piracy/drug smuggling/Ilegal Immigration [Personal Interview]	2 =TOA Brightness Temp	~15m	Lat.: 60º N to 35º S Lon. 70º W to 70º E			Two dimensional MRTD models	1 band: 0.8 - 2.5 µm	SAR, VIS	AIS
Industrial/power plant monitoring [Wu et al. 2007; Tang et al. 2003]	3 = Surface Temp	10-15m			1-2 K	TES, models, statistics	Spectrometry	UV/VIS/NIR	Sonde Measurements
Trafficability (off-road soil moisture content) [Personal Interview]	3 = Surface Temp	30m			1-2 K	TTM	Two bands (10 – 12 µm)	SAR	DEM, ECMWF, LSE

FUEGOSAT SYNTHESIS STUDY (1-6101/09/NL/BJ)

TIR remote sensing applications selected after the consolidation review (workshop) and priority level

Topic	Subtopic	Application	Priority
Land & Solid Earth	Volcanoes	Eruption clouds-ash	Medium
		Degassing plumes	High
		Hot spots and active lava flows	High
	Fires	Detection of fires	Medium
		Estimation of fire risk	High
		Estimation of burnt area	Medium
	Water management	Detection of water stress in crops (tree crops)	Medium
		Detection of water stress in crops (typical crops)	High
		Detection of water stress in forest	High
		Detection of evapotranspiration in crops (tree crops)	Medium
		Detection of evapotranspiration in crops (typical crops)	High
		Detection of evapotranspiration in River Basin	High
		Detection of evapotranspiration in continents	Medium
	Coal mine fires	Detection of coal mine fires	High
		Delineation of potential coal fires and coal fire risk areas	Medium
	Geology	Soil composition	High
Health & Hazards	Urban Heat Island	Vegetation maps	High
		Land cover/Land Use	High
		Building Information	Medium
		Air Quality	Medium
	Industrial risks	Air pollution	Medium
		Differentiate between urban and industrial zone	High
		Oil spill detection	Low
		Plume detection	Medium
	Coastal inundations	Prediction of floods	Low
		Monitoring of floods	Medium
		Asbestos-cement detection over non-accesible areas	Low
Security & Surveillance		Detection of minefields	Low
		Border Security	Medium
		Target activity monitoring	Medium
	Ship/Port monitoring	Piracy/drug smuggling/Ilegal Immigration	Medium
		Industrial/power plant monitoring	Medium
		Trafficability (off-road soil moisture content)	Medium

LST/Emissivity Focus Area Products List

Emissivity

Emissivity, derived from Terra ASTER
Contact: Alan Gillespie
Institution: JPL
Link to validation information

Spatial Coverage: global
Temporal Coverage: 2000+
Spatial Scale: 90 m
Temporal Scale: 16-day

Emissivity, derived from Terra ASTER
Contact: Simon Hook
Institution: JPL
Link to validation information

Spatial Coverage: North America
Temporal Coverage: 2000-2009
Spatial Scale: 100 m
Temporal Scale: Seasonal

Land Surface Temperature

Land Surface Temperature, derived from Meteosat (MSG)
Contact: User Services
Institution: POSTEL

Spatial Coverage: Europe + Africa
Temporal Coverage: 1996-2003
Spatial Scale: 50 km
Temporal Scale: 10-day

Land Surface Temperature (LST), derived from Meteosat (MVIRI)
Contact: Folke Olesen
Institution: Karlsruhe Institute of Technology
Link to validation information

Spatial Coverage: Europe + Africa
Temporal Coverage: 1999-2005
Spatial Scale: 5 km
Temporal Scale: 30 min

Land Surface Temperature (LST), derived from Terra ASTER
Contact: Alan Gillespie
Institution: JPL
Link to validation information

Spatial Coverage: global
Temporal Coverage: 2000+
Spatial Scale: 90 m
Temporal Scale: 16-day

Land Surface Temperature (LST), derived from ENVISAT AATSR
Contact: EO Helpdesk
Institution: ESA
Link to validation information

Spatial Coverage: global
Temporal Coverage: 2002+
Spatial Scale: 1 km
Temporal Scale: Daily

Land Surface Temperature (LST)/Emissivity, derived from Aqua AIRS
Contact: Joel Susskind
Institution: NASA
Link to validation information

Spatial Coverage: global
Temporal Coverage: 2002+
Spatial Scale: 50 km
Temporal Scale: Daily

Land Surface Temperature, derived from Meteosat (MSG) SEVIRI
Contact: Help Desk
Institution: LandSAF
Link to validation information

Spatial Coverage: Europe, Africa, S. America
Temporal Coverage: 2006-2009
Spatial Scale: 3 km
Temporal Scale: 15-min

Land Surface Temperature and Emissivity

Land Surface Temperature (LST)/Emissivity, derived from Terra/Aqua MODIS
Contact: Zhengming Wan
Institution: UCSB
Link to validation information

Spatial Coverage: global
Temporal Coverage: 2000+
Spatial Scale: 0.5 deg
Temporal Scale: 8-day

Land Surface Temperature (LST)/Emissivity, derived from Terra/Aqua MODIS
Contact: Zhengming Wan
Institution: UCSB
Link to validation information

Spatial Coverage: global
Temporal Coverage: 2000+
Spatial Scale: 0.5 deg
Temporal Scale: Daily

Land Surface Temperature (LST)/Emissivity, derived from Terra/Aqua MODIS
Contact: Zhengming Wan
Institution: UCSB
Link to validation information

Spatial Coverage: global
Temporal Coverage: 2000+
Spatial Scale: 0.5 deg
Temporal Scale: Monthly

Land Surface Temperature (LST)/Emissivity, derived from Terra/Aqua MODIS
Contact: Zhengming Wan
Institution: UCSB
Link to validation information

Spatial Coverage: global
Temporal Coverage: 2000+
Spatial Scale: 1 km
Temporal Scale: 8-day

Land Surface Temperature (LST)/Emissivity, derived from Terra/Aqua MODIS
Contact: Zhengming Wan
Institution: UCSB
Link to validation information

Spatial Coverage: global
Temporal Coverage: 2000+
Spatial Scale: 1 km
Temporal Scale: Daily

Land Surface Temperature (LST)/Emissivity, derived from Terra/Aqua MODIS
Contact: Zhengming Wan
Institution: UCSB
Link to validation information

Spatial Coverage: global
Temporal Coverage: 2000+
Spatial Scale: 5 km
Temporal Scale: Daily

CEOS WGCV LPV– LST and Emissivity

The main objective is the calibration and validation of OPERATIONAL PRODUCTS

Datasets

Compilation of dataset and delivery

Campaign Justification Report

DATASETS: ground data with airborne and satellite data

High spatial resolution sensors (AHS, ASTER, INGENIO, Sentinel2)

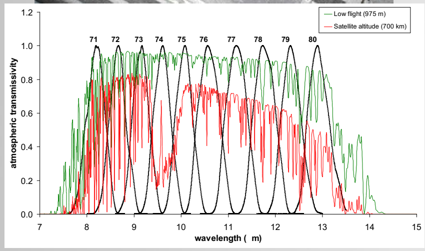

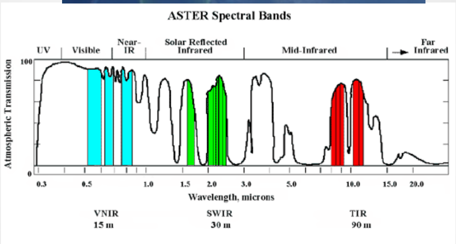

Low spatial resolution sensors (MODIS, AVHRR, AATSR, Sentinel3)

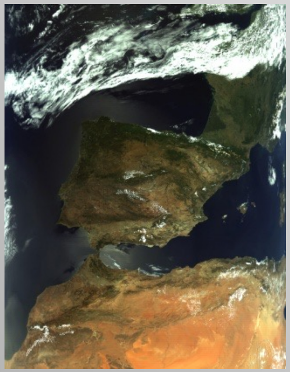

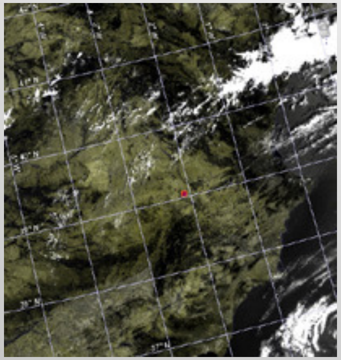

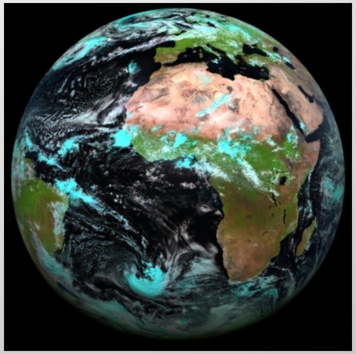

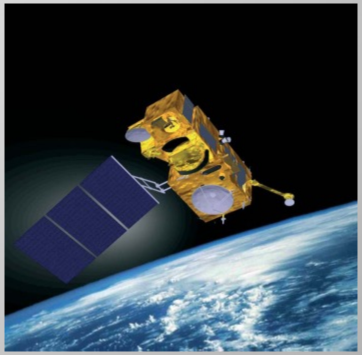

esa Earthnet Online

European Space Agency

EO Data Access
How to Apply
How to Access
Earthnet Online
Services
Site Map
Frequently asked questions
Glossary
Credits
Terms of use
Contact us
Search
Go
Advanced Search

ESA Earth Observation Campaigns Data

- The datasets resulting from ESA airborne car can be accessed by submitting a request on t website
- For additional information, please contact the
- Back to ESA Earth Observation Campaigns D

Campaign (with link to final report PDF)	Year	Geographic site(s)	Field of applicatio
TropiSAR	2009	Nouragues, Paracou (French Guiana)	Tropical f biomass r using L- a P-Band S
THERMOPOLIS	2009	City of Athens (Greece)	Urban He Islands (Multispe Thermal I
SEN3EXP	2009	Boussole (F), San Rossore (I), Venice AAOT(I), Barrax (E)	Ocean, fo and cultiv areas in s to Sentin mission
BIOSAR-2	2008	Krycklan (Sweden)	Forest Bic Mapping u and P-bar
POLARIS Proof-of-Concept	2008	Greenland	P-Band ic sounding
DESIREX	2008	City of Madrid (Spain)	Urban He Islands (Multispe Thermal I
CEFLES2	2007	Les Landes (France)	Urban, fo cultivated burned ar support to

AGRISAR	2006	site (Western Pomerania, D)	Agriculture		2 HDs	esa wpp-279
EAGLE	2006	Cabauw, Loobos, Speul derbos (NL)	Natural Vegetation (Grassland and Forest)		1 HD	esa wpp-279
AIRFIRE	2006	Central Italy	Forest and bushes fire monitoring		3 DVDs	
AQUI FEREX	2005	Ben Gardane, Gabes (Tunisia)	Soil moisture, land use, land cover classification		1 HD, 4 DVDs	
SEN2 FLEX	2005	Barrax (E)	Agriculture		1 HD	esa wpp-271
WALEX	2005	Indian Ocean and Micronesia	Atmosphere	YES, click here	1 CD	
BAC CHUS -DOC	2005	Frascati (I)	Agriculture		9 DVDs	
INDREX-2	2004	Kalimantan (Borneo), Indonesia	X-, C-, L- and P-Band SAR over Tropical Forest		2 HDs	
DOMEX -1	2004	Dome-Concordia (Antarctica)	SMOS	YES, click here	1 CD	
SPARC	2003-2004	Barrax (E)	Agriculture		14 DVDs, 1 HD, 2 CDs	esa wpp-250
Terra SARSim	2003	Barrax (E)	Agriculture		1 CD + 48 DVDs	
Cryovex	2003	Greenland, Svalbard	Sea-ice & Inland ice		5 DVDs	
WALEX	2002	North & Middle Atlantic	Atmosphere	YES, click here	1 CD	
SIFLEX	2002	Sodankyla (FIN)	Forest fluorescence	YES, click here	1 DVD	
ESAG	2002	Greenland, Svalbard	Gravity field		47 CDs	
LaRa	2002	Greenland, Svalbard	Ice-sheets & sea ice		1 hard disk	

Campaign Elements

Example SEN3EXP

- **Data set comprising**
  - Satellite data from MERIS & AATSR, complemented with Chris, MODIS, ASTER, SeaWiFS; MERIS spectral campaign
  - Airborne data, covering in hyperspectral mode the VIS, NIR, SWIR and TIR spectral range (CASI1500, SASI600, AHS)
  - Ground measurements
- **4 experimental sites**
  - Barrax: various agriculture vegetation types
  - San Rossore: coniferous forest and other forest types
  - Boussole: Case 1 water
  - AAOT: Case 1 and Case 2 water
- **Data processing**
  - Calibration of MERIS spectral campaign
  - Atmospheric correction of airborne data
  - Transportation of airborne data to top of atmosphere
  - Simulating Sentinel 3 data with MERIS, AATSR and airborne data

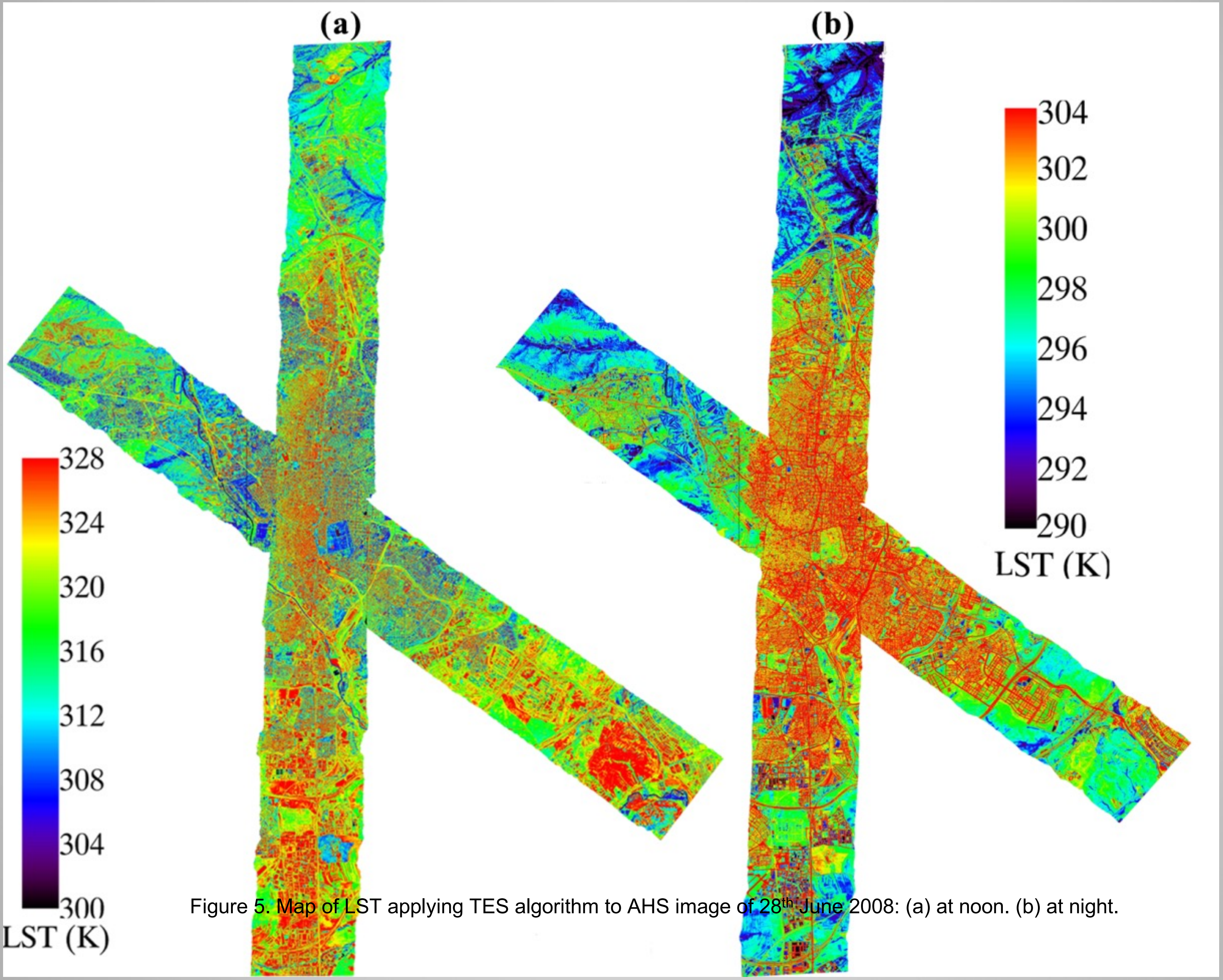

Figure 5. Map of LST applying TES algorithm to AHS image of 28th June 2008: (a) at noon. (b) at night.

Barrax Campaign

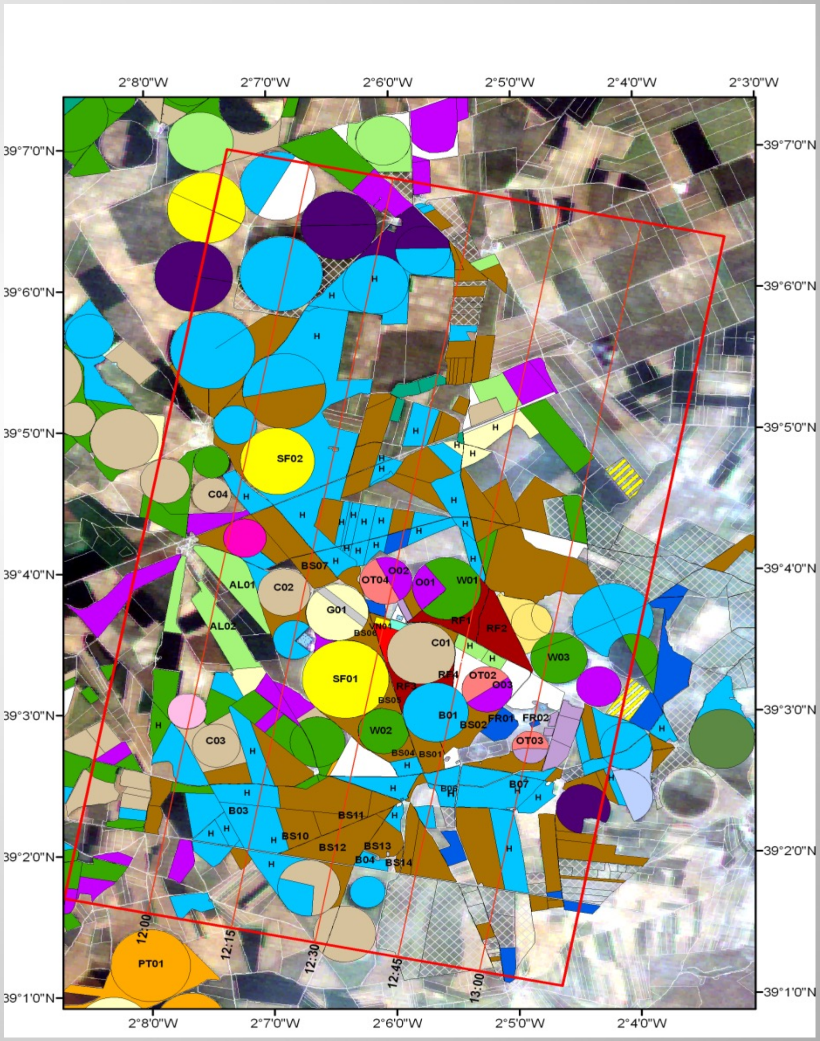

Ground data:

Calibration → Brightness Temperature (T_B)

Validation → Surface temperature (T_s) and emissivity (ε)

Instrumentation for Thermal Radiometric Measurements:

- -Single and multiband radiometers
- -Different FOV
- -Thermal Cameras
- -Calibration sources

				
	EVEREST 3000	OPTRIS CS	RAYTEK MID	NEC TH7800
				
CIMEL CE 312-1& 2	APOGEE IRR-P	OPTRIS CT-LT15	RAYTEK ST6 & ST8	NEC TH9100
				
HEITRONICS KT 19.85	REFLECTANC E PLATE	LAND P80P	EVEREST 1000	FLIR P640

intercomparison with LST products

(E.g. CEFLES-2 campaign, 2007)

AATSR LST image retrieved 27 july 2007 (21:25 UTC) with SW6 algorithm proposed

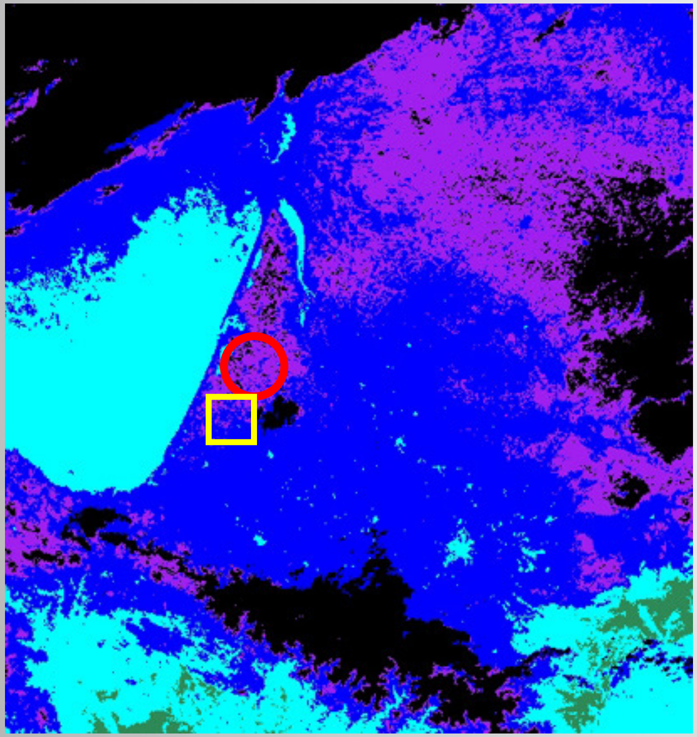

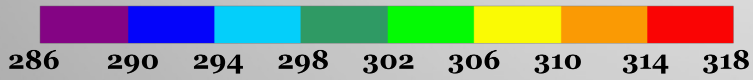

AATSR LST Level 2 product 27 july 2007 (21:25 UTC)

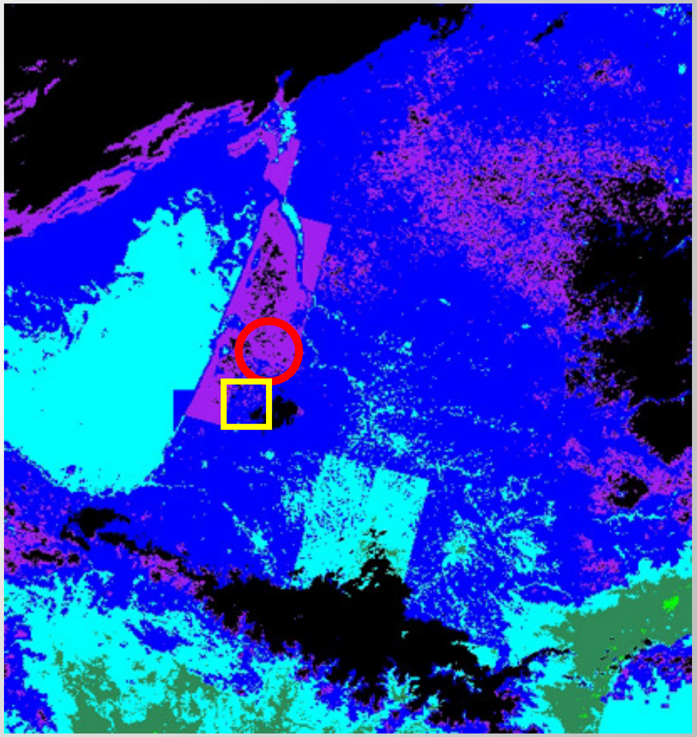

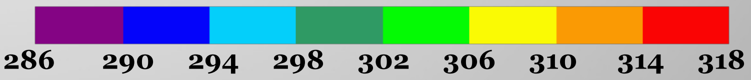

intercomparison with LST products

(E.g. CEFLES-2 campaign, 2007)

MODIS LST image retrieved 26 july 2007 (10:38 UTC) with SW algorithm from GCU

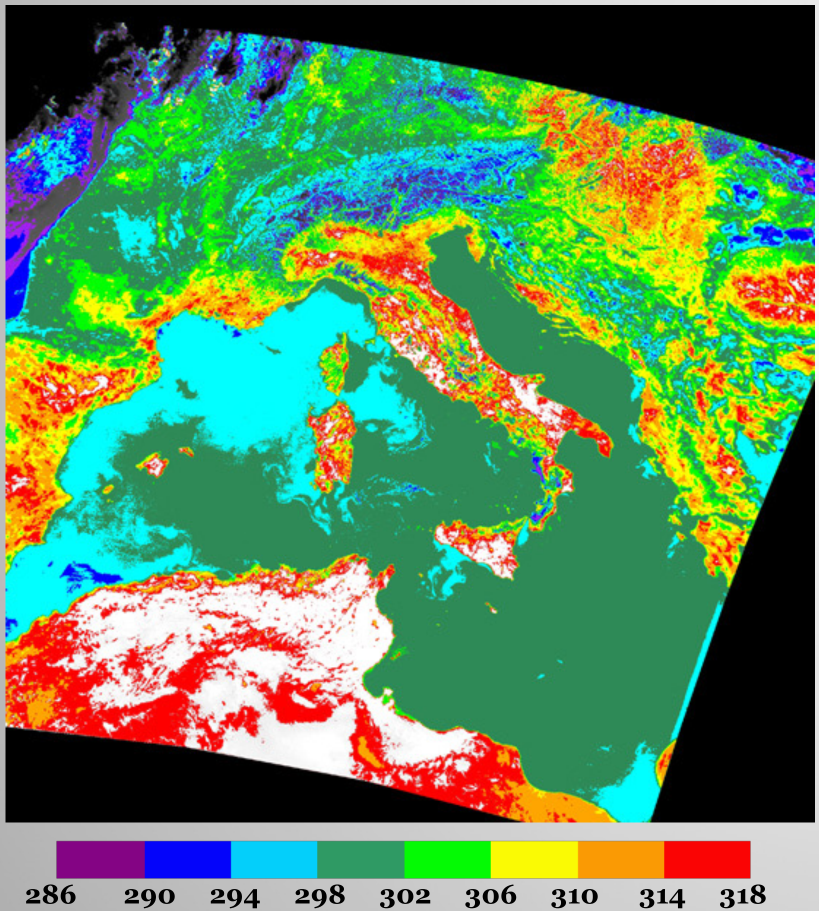

MODIS LST product 26 july 2007 (10:38 UTC) from EOS Data Gateway

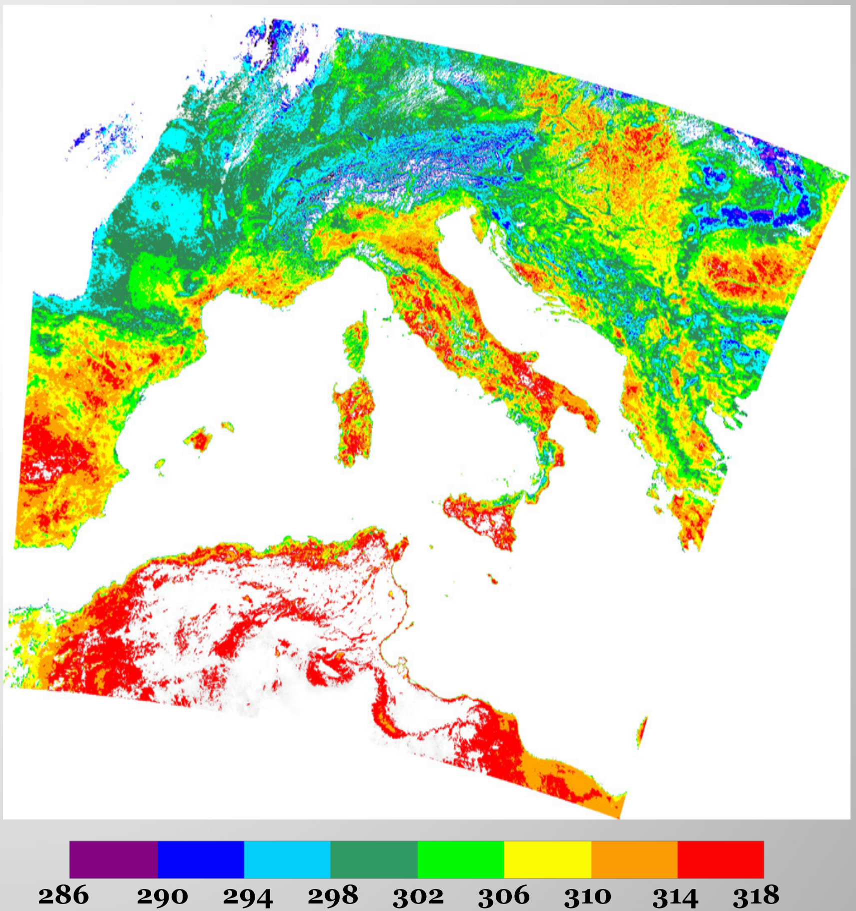

intercomparison with LST products

(E.g. CEFLES-2 campaign, 2007)

SEVIRI LST image retrieved with SW algorithm from GCU

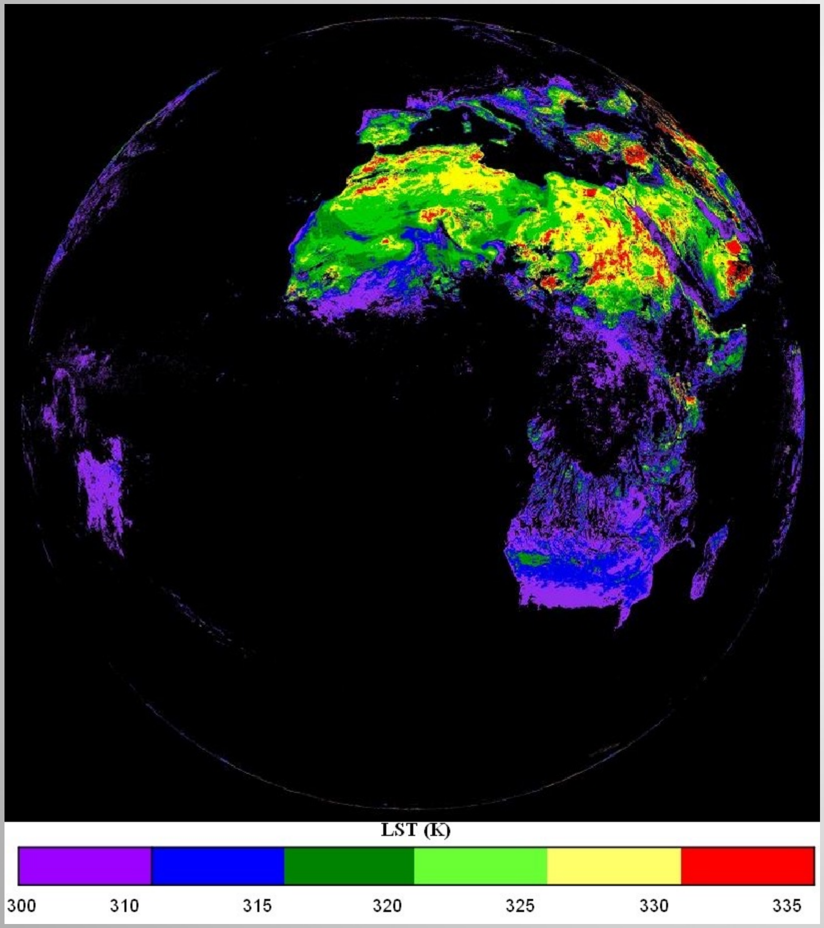

SEVIRI LST products from LandSAF

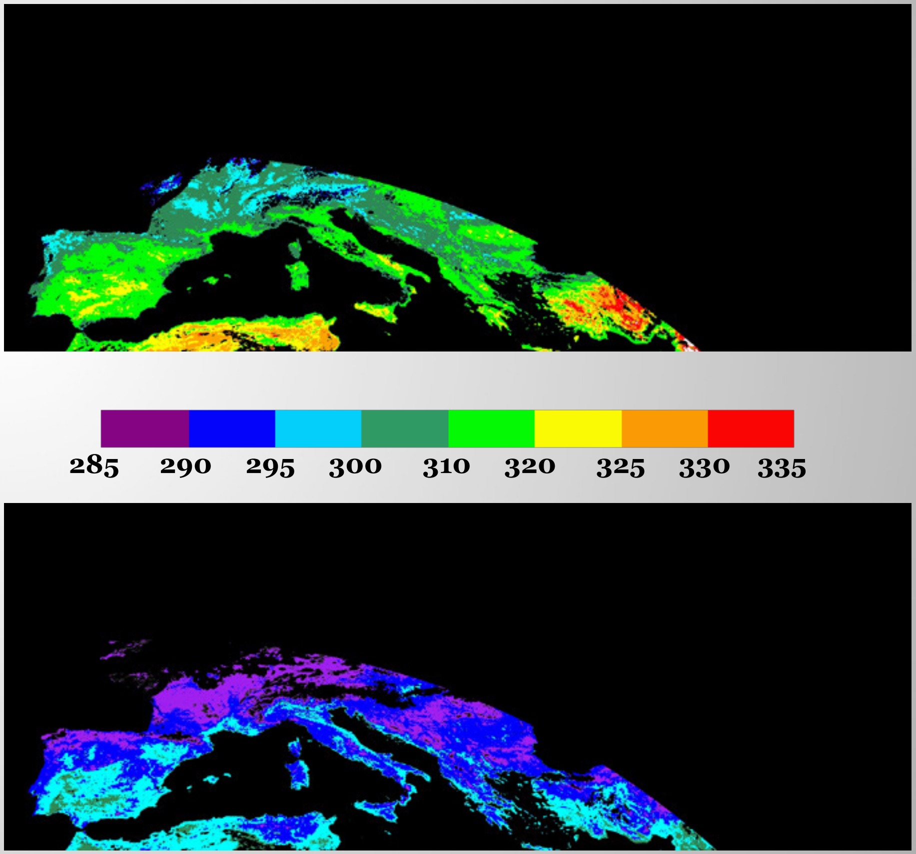

intercomparison with LST products

(E.g. CEFLES-2 campaign, 2007)

AATSR

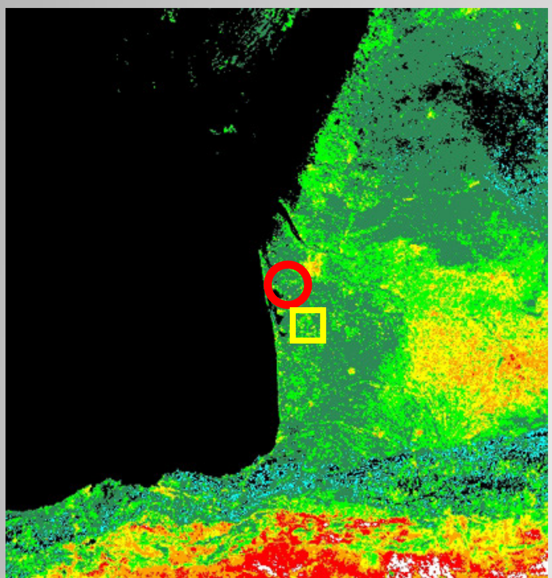

MODIS

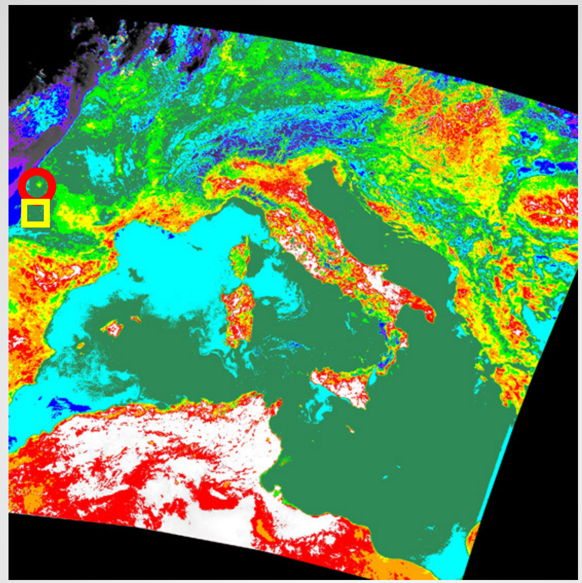

SEVIRI

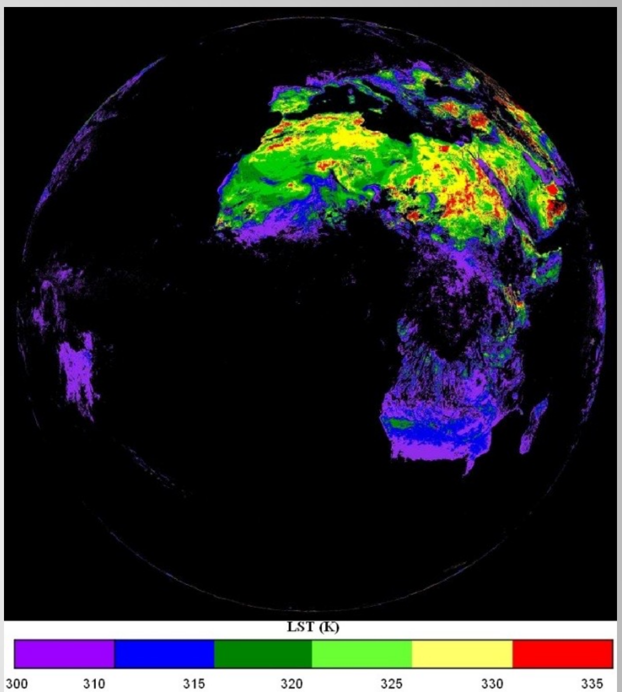

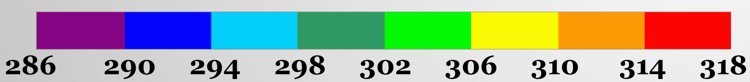

Area of 3x3 pixel size (1km pixel)

Area of 1 pixel size (3km pixel)

300.0	299.2	300.1
300.6	300.1	308.5
303.3	302.9	309.2

301.9	300.1	300.1
302.2	300.9	300.0
300.7	298.9	300.0

300.6	300.5	300.4
301.5	301.3	301.2
301.4	302.0	301.6

300.4	300.2	300.1
300.1	299.9	299.7
299.9	299.8	299.5

Mean value of the 3x3 pixel area

302.7 **300.5** **301.2** **299.9** **302.5** **301.7**

intercomparison with LST products

(E.g. CEFLES-2 campaign, 2007)

*Difference with channel 11 brightness temperature

** MODIS (22:05h)

	DAY		NIGHT	
	26th 1st area	26th 2nd area	27 1st area	27 2nd area
LST AATSR SW (K)	302.7	300.5	289.7	289.8
AATSR SW – AATSR Level2	Not Processed (4.9)*	-2.4	Not Processed (2.5)*	-1.0
AATSR SW – SEVIRI SW	0.2	-1.2	1.3	0.4
AATSR SW – SEVIRI LandSAF	0.0	-0.2	1.8	0.2
AATSR SW – MODIS SW	1.5	0.6	0.5	0.3
AATSR SW – MODIS EOS data	3.0	2.3	0.9	Not Processed**
AATSR SW – IN SITU	-0.8	-	0.0	-

Low and negative BIAS (-0.6 K)
Standard deviation around 1 K
RMSE lower than 1.5 K

Intercomparison of algorithms

Site	Date	W (g/cm^2)	Plot	LST_{situ} (K)	LST_{RTE} (K)	LST_{SW} (K)	LST_{SC} (K)	D_{RTE} (K)	D_{SW} (K)	D_{SC} (K)
Calibration Points										
Barrax	23/05	1.1	Wheat	291.8	-	-	-	-	-	-
Doñana	22/06	3.2	Marsh	304.7	-	-	-	-	-	-
Validation Points										
Barrax	01/06	1.0	Wheat	292.8	292.3	291.4	292.4	-0.5	-1.4	-0.3
	24/06	1.4	Wheat	303.8	303.3	302.3	303.7	-0.4	-1.5	-0.1
	12/09	1.8	Corn	295.1	296.1	295.5	295.9	1.0	0.4	0.8
	12/09	1.8	Soil	301.1	301.0	300.0	300.8	-0.1	-1.0	-0.3
	12/09	1.8	Soil	302.6	301.8	301.6	301.6	-0.8	-1.0	-1.0
Doñana	19/04	2.0	Marsh	297.6	296.4	298.0	295.1	-1.2	0.4	-2.5
	05/05	1.7	Marsh	297.6	298.1	297.8	297.6	0.5	0.2	0.0
							Bias	-0.2	-0.6	-0.5
							SD	0.8	0.8	1.0
							RMSE	0.8	1.0	1.2

Calibration and Validation activities

Cal/Val is a key activity in order to ensure the collection of data with good quality. Validation is required in order to check the accuracy of the delivered products.

State of the art of LST validation

Much of the international effort on validating data from spaceborne thermal infrared instruments has focused on SST. In comparison, the validation activities for LST are carried out by a fairly small research community. The following describes some of the more recent LST validation activities for AATSR, MODIS, and SEVIRI.

AATSR

Initial validation of the AATSR (Sobrino et al 1996, Soria et al 2002) product was carried out over several Australian field sites (Prata, 2003) and it was found that the accuracy of the algorithm is within the target specification. More recently, LST derived from AATSR was further validated over Valencia, Spain and Lake Tahoe, CA/NV, USA (Coll, Hook, et al., 2009), finding nearly zero average biases and standard deviations of 0.4 – 0.5 K for both daytime and nighttime data. Both of these studies indicate the need for higher-resolution auxiliary to be used within the operational AATSR LST algorithm. The operational AATSR LST product was validated over Morocco where average biases of -1.00 K and -1.74 K were found for daytime and nighttime data, respectively (Noyes et al., 2007).

MODIS

Initial validation of MODIS (Justice et al., 1998) LST was carried out at multiple validation sites indicating that MODIS LSTs agree with in situ LSTs within ±1 K (Wan et al., 2002, 2004). Other studies using long-term nighttime ground measurements have found biases of 0.8 K for some sites and up to -3 K for other sites (Wang et al., 2008). Validation of the MODIS V5 level 2 LST product was further carried out in Valencia, Spain and Hainich, Germany, using both temperature- and radiance-based validation techniques (Coll, Wan, et al., 2009). The results indicate an average bias of -0.3 K and an RMSE of ±0.7 K for the temperature-based validation.

MSG-SEVIRI

The SEVIRI (Aminou, 2002) LST product provided by the facility on land surface analysis (LAND-SAF) has been validated against the MODIS LST product and against in situ observations made at the Evora station in Portugal, finding nighttime differences for the latter of 1-2 K, and higher discrepancies for daytime comparisons (Trigo et al., 2008). More recently, the uncertainty of LST from SEVIRI was assessed over the Gobabeb validation site in Namibia, where RMS difference between 1 K and 2 K were found (Freitas et al., 2010).

Vicarious Calibration

The predicted at-sensor radiance (or brightness temperature) for each thermal band (using field measurements and MODTRAN) must be compared with the measured radiance in this band.

Theoretical Basis: Temperature-Based Method

The at-sensor radiance for each band (i) is predicted from measured surface kinetic temperatures and radiative transfer codes (MODTRAN):

$$L_i^{at-sensor} = \left[\varepsilon_i B_i(Ts) + (1-\varepsilon_i) L_i^{\downarrow} \right] \tau_i + L_i^{\uparrow}$$

ε: surface emissivity
B: Planck function
T_s: surface kinetic temperature (LST)
$L^{\downarrow}$: atmospheric downwelling radiance
τ: atmospheric transmissivity
$L^{\uparrow}$: path radiance

(Each spectral magnitud is convolved using the filter functions)

T_s : measured in situ
ε_i : emissivity values have been extracted from spectral libraries
τ, $F^{\downarrow}$, $L^{\uparrow}$: calculated from atmospheric soundings by using MODTRAN-4.

FIELD-BASED MEASUREMENTS

MEASUREMENTS: EMISSION

At ground level, the atmospheric layer between the surface and the sensor is negligible

$$\tau_i \approx 1 \quad L_i^{\uparrow} \approx 0$$

$$L_i^{at-sensor} = \left[\varepsilon_i B_i(Ts) + (1-\varepsilon_i) L_i^{\downarrow} \right] \tau_i + L_i^{\uparrow} \Rightarrow L_i^{radiometer} = \varepsilon_i B_i(Ts) + (1-\varepsilon_i) L_i^{\downarrow}$$

If we measure ε and $L^{\downarrow}$, we can obtain Ts:

$$B_i(Ts) = \frac{L_i^{radiometer} - (1-\varepsilon_i) L_i^{\downarrow}}{\varepsilon_i}$$

If we measure Ts and $L^{\downarrow}$, we can obtain ε:

$$\varepsilon_i = \frac{L_i^{radiometer} - L_i^{\downarrow}}{B_i(Ts) - L_i^{\downarrow}}$$

Vicarious calibration

- Significant bias (around 3 K) between Landsat-8 derived data and measured values of LST.
- Result later confirmed by the announcement published in the USGS Landsat mission web page on September 16, 2013.
- 2 points for calibration (extreme data points, the lowest and highest radiance)

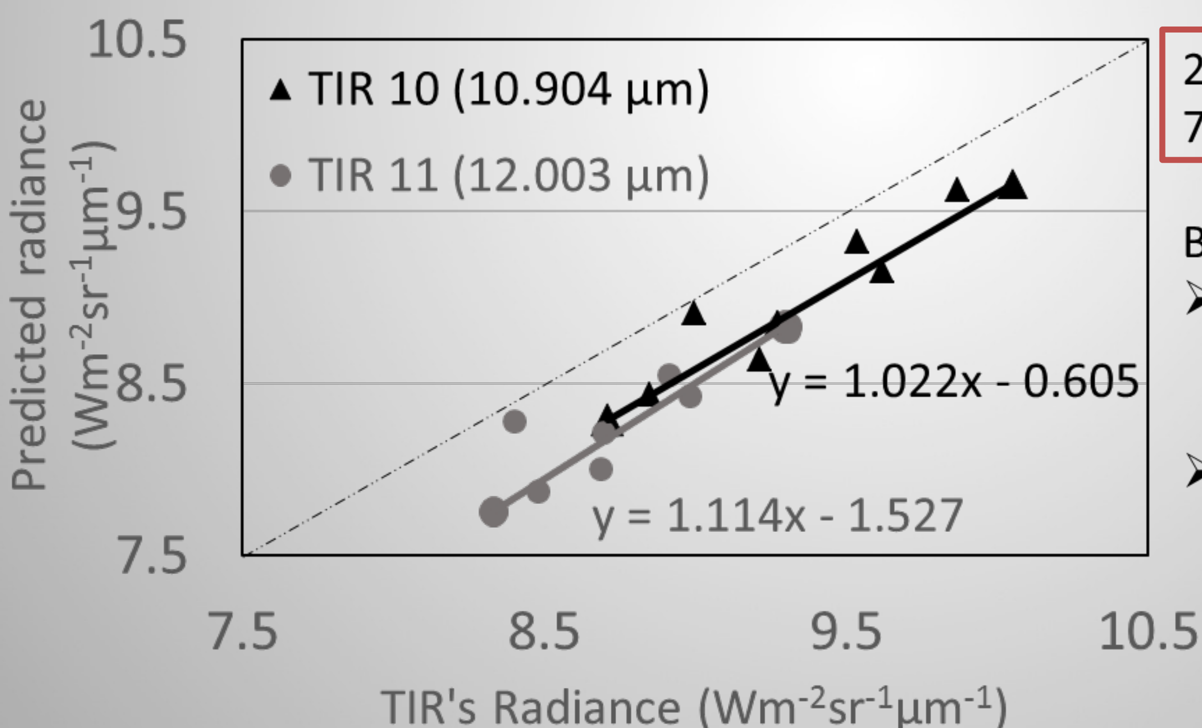

2 points for calibration
7 points for validation

Bias estimated at 300 K.

- TIRS 1 negative bias: ~0.4 $W \cdot m^{-2} \cdot sr^{-1} \cdot \mu m^{-1}$ ~2.6 K
- TIRS 2 negative bias: ~0.6 $W \cdot m^{-2} \cdot sr^{-1} \cdot \mu m^{-1}$ ~4.8 K

Calibration (day flight)

- Only one pass is shown (**south-north**)
- Points of calibration: **Green Grass** and **Water**
- AHS curve and in situ curve fit good
- No band with wrong results

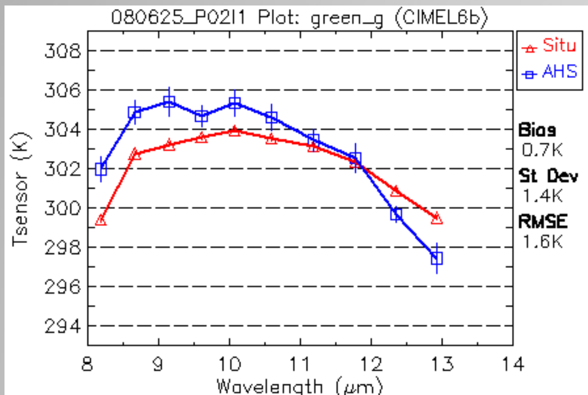

25 June, 11:27
Cimel
Green Grass

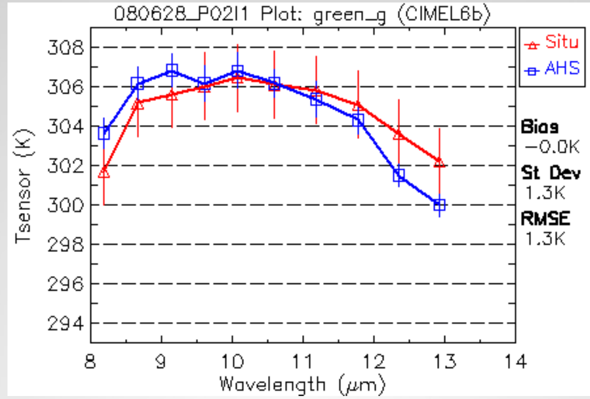

28 June, 11:53
Cimel
Green Grass

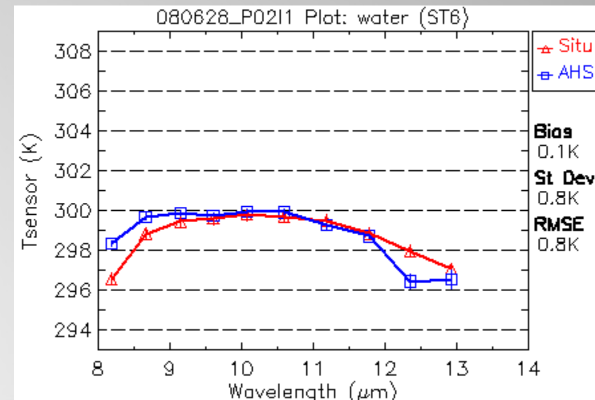

28 June, 11:53
Raytech ST6
Water

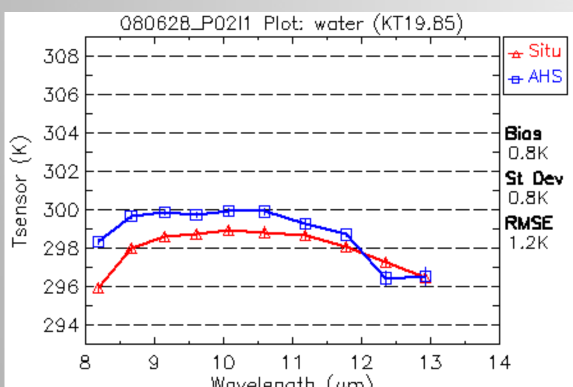

28 June, 11:53
Heitronics KT19.85
Water

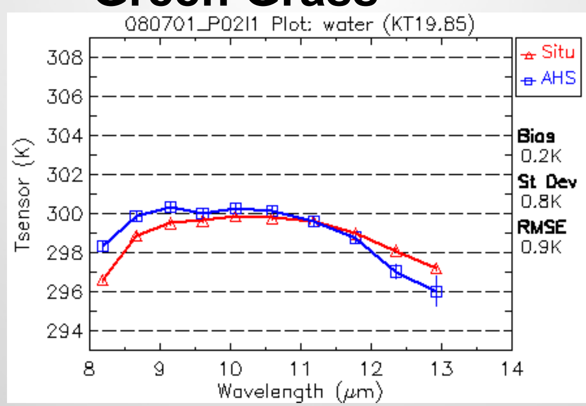

01 July, 11:44
Heitronics KT19.85
Water

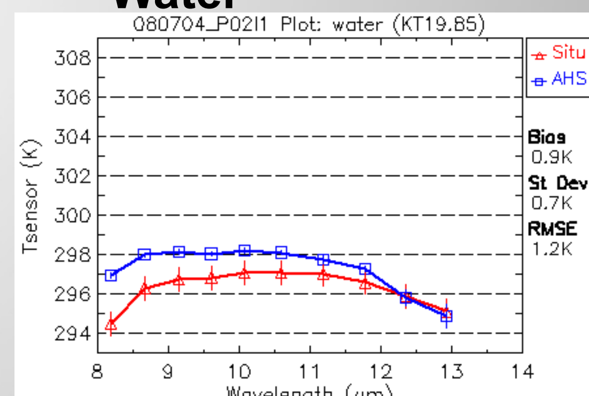

04 July, 11:32
Heitronics KT19.85
Water

Calibration (night flight)

- Only one pass is analized (**south-north**)
- Points of calibration: Green Grass and Water
- AHS curve and in situ curve fit good
- No band with wrong results

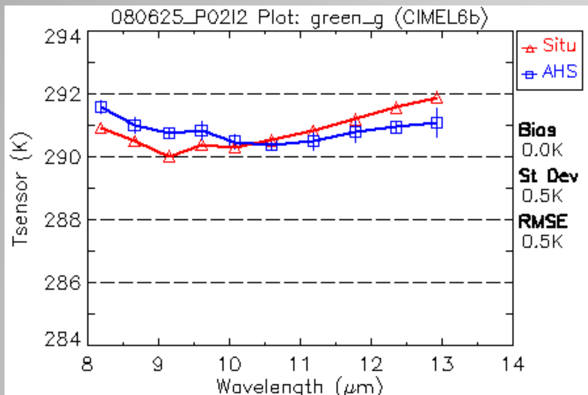

25 June, 22:31
Cimel
Green Grass

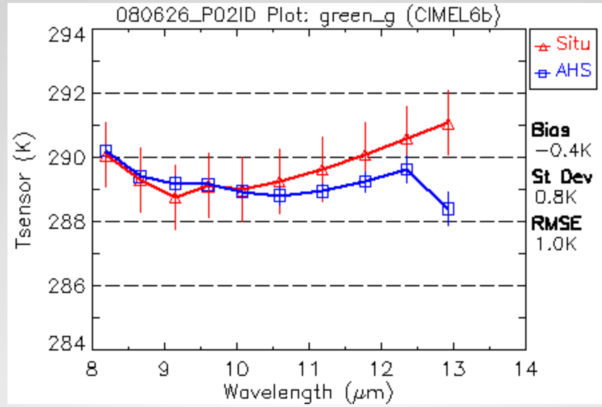

26 June, 04:26
Cimel
Green Grass

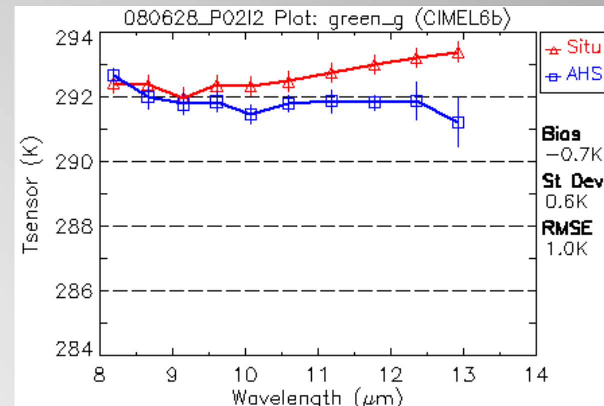

28 June, 21:44
Cimel
Green Grass

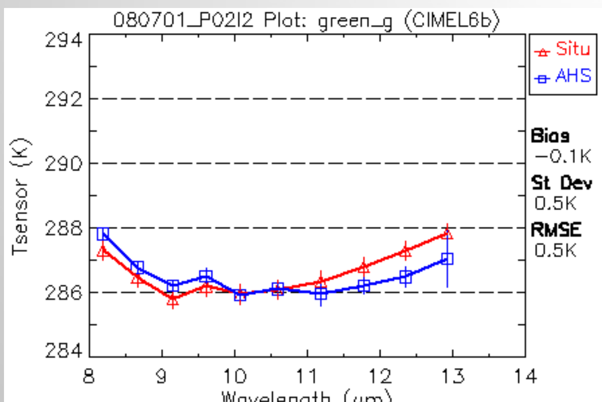

01 July, 22:12
Cimel
Green Grass

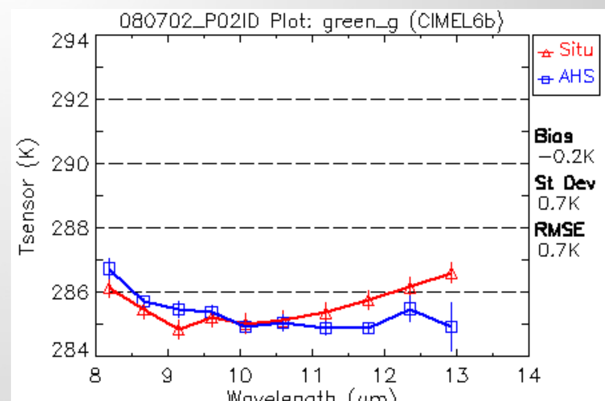

02 July, 04:26
Cimel
Green Grass

Calibration

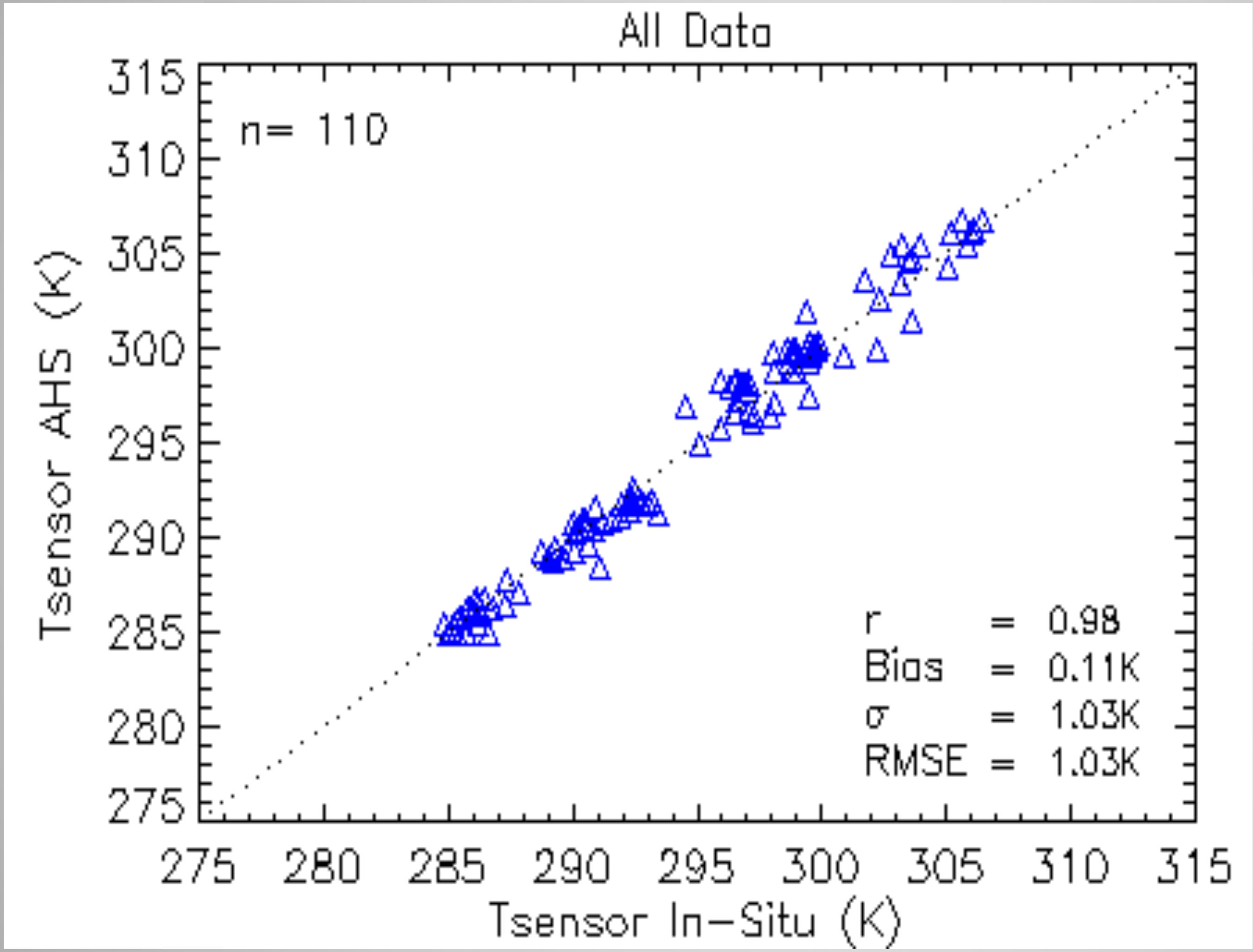

r = 0.98
RMSE = 1 K

Improvements?

SEN4LST RETRIEVAL SCHEME

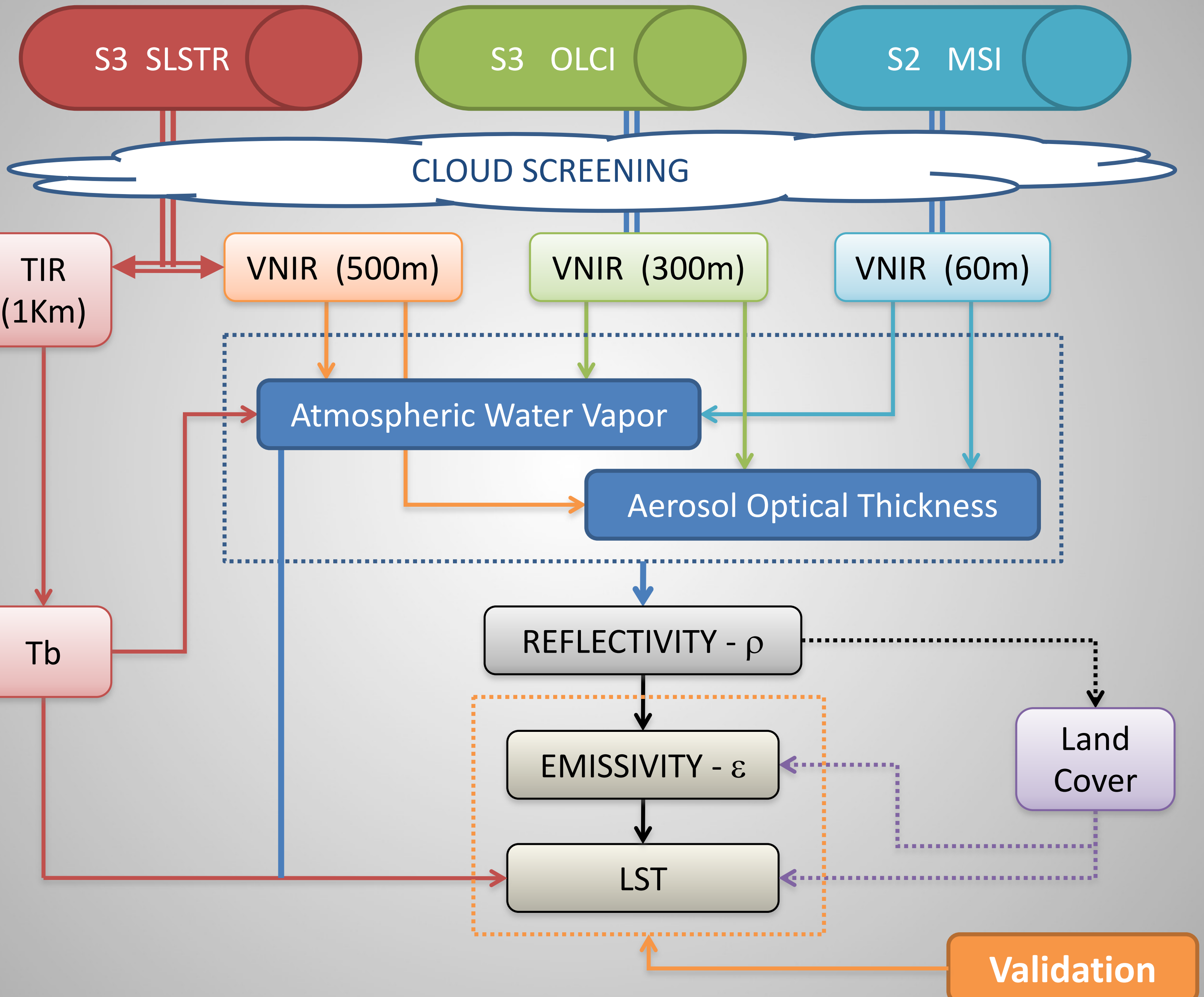

ALGORITHMS

Radiative Transfer Equation (RTE)

With the thermal radiance measured at-sensor level and the atmospheric parameters obtained with radiosounding, a LST can be retrieved.

$$L_{sen} = \left[\varepsilon B_{T_S} + (1-\varepsilon)L_d\right]\tau + L_u$$

Applying the inverse of the Planck's law

$$T_S = \frac{c_2}{\lambda \ln\left\{\dfrac{c_1}{\lambda^5\left[\dfrac{L_{sen} - L_u - \tau(1-\varepsilon)L_d}{\tau\varepsilon}\right]} + 1\right\}}$$

$\mathbf{c_1}$ = 1.19104·10^{8} W·µm^{4}·m^{-2}·sr^{-1}

$\mathbf{c_2}$ = 14387.7 µm·K

$\boldsymbol{L_{sen}}$: Thermal radiance at sensor level

$\boldsymbol{B_{T_S}}$: Radiance of Planck's law

$\boldsymbol{T_S}$: Land surface temperature

$\boldsymbol{\varepsilon}$: Land Surface Emissivity (LSE)

$\boldsymbol{\tau}$: Atmospheric transmissivity

$\boldsymbol{L_u}$: Up-welling atmospheric radiance

$\boldsymbol{L_d}$: Down-welling atmospheric radiance

$\boldsymbol{\lambda}$: Effective band wavelength

ALGORITHMS

Single-Channel (SC) algorithm

The practical approach proposed in the SC algorithm consists of the approximation of the atmospheric functions defined by Ψ_1, Ψ_2, Ψ_3 versus the atmospheric water vapour content W from a second order polynomial fit.

$$T_s = \gamma\left[\frac{1}{\varepsilon}\left(\psi_1 L_{sen} + \psi_2\right) + \psi_3\right] + \delta$$

- Can be applied to any of the two TIRS bands. (Preferably to TIRS 1)
- Only requires the knowledge of *w*. Jiménez-Muñoz et al. (2009)

$\boldsymbol{L_{sen}}$: Thermal radiance at sensor level

$\boldsymbol{T_S}$: Land surface temperature

$\boldsymbol{T_{sen}}$: At-sensor brightness temperature

$\boldsymbol{b_\gamma}$: (1324 K for TIRS-1, and 1199 K for TIRS-2)

$\boldsymbol{\Psi_1, \Psi_2, \Psi_3}$: Atmospheric functions

$\boldsymbol{w}$: Water vapour (Radiosoundings, MOD07, in situ data…)

$$\gamma \approx \frac{T_{sen}^2}{b_\gamma L_{sen}} \quad \psi_1 = \frac{1}{\tau}; \quad \psi_2 = -L_d - \frac{L_u}{\tau}; \quad \psi_3 = L_d$$

$$\delta \approx T_{sen} - \frac{T_{sen}^2}{b_\gamma}$$

$$\begin{bmatrix} \psi_1 \\ \psi_2 \\ \psi_3 \end{bmatrix} = \begin{bmatrix} c_{11} & c_{12} & c_{13} \\ c_{21} & c_{22} & c_{23} \\ c_{31} & c_{32} & c_{33} \end{bmatrix} \begin{bmatrix} w^2 \\ w \\ 1 \end{bmatrix}$$

$$C = \begin{bmatrix} 0.04019 & 0.02916 & 1.01523 \\ -0.38333 & -1.50294 & 0.20324 \\ 0.00918 & 1.36072 & -0.27514 \end{bmatrix}$$

ALGORITHMS

Split-Window (SW) algorithm

The basis of the technique is that the radiance attenuation for atmospheric absorption is proportional to the radiance difference of simultaneous measurements at two different wavelengths. Sobrino et al. (1996)

$$T_s = T_i + c_1(T_i - T_j) + c_2(T_i - T_j)^2 + c_0 + (c_3 + c_4 w)(1 - \varepsilon) + (c_5 + c_6 w)\Delta\varepsilon$$

Emissivity's extracted from ASTER spectral library

$\varepsilon = 0.5\ (\varepsilon_i + \varepsilon_j)$ $\Delta\varepsilon = (\varepsilon_i - \varepsilon_j)$

c_0 = -0.268; c_1 = 1.378; c_2 = 0.183; c_3 = 54.30; c_4 = -2.238; c_5 = -129.20 ; c_6 = 16.40

$\boldsymbol{T_S}$: Land surface temperature

$\boldsymbol{T_i}, \boldsymbol{T_j}$: At-sensor brightness temperature at bands *i* and *j*

ALGORITHM SENSITIVITY ANALYSIS (K)	
δ_{alg}	0.6
$\delta_{NE\Delta T}$	1.5 (0.4)
δ_{ε}	0.6
δ_{w}	0.1

→ ***e(LST) = 2.1 (1.5)***

- The Split-Window technique uses two TIR bands typically located in the atmospheric window between 10 and 12 µm
- Similar to the SC algorithm, the SW algorithm only requires the knowledge of *w*.

Temperature and Emissivity Separation (TES)

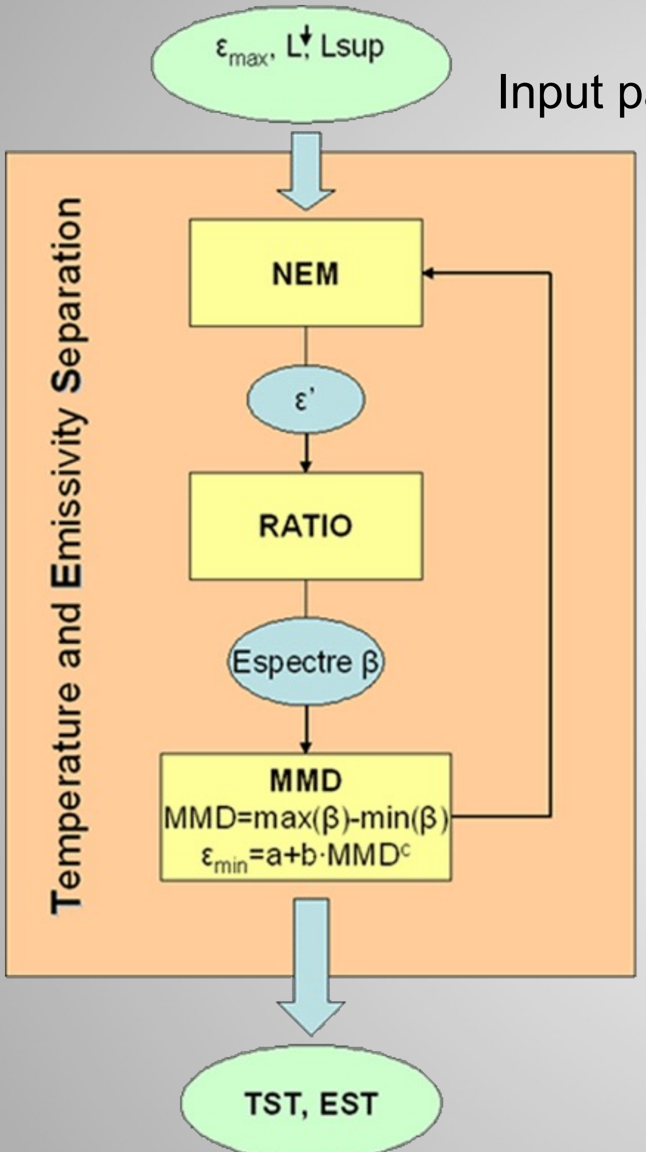

Input parameters: $L_i^{\sup}$ $L_i^{atm\downarrow}$ $\varepsilon_{\max}$ (initial emissivity)*

$$R_i' = L_i^{\sup} - \left(1 - \varepsilon_{\max}\right) L_i^{atm\downarrow}$$

$$T' = \max\left(T_i\right); \quad T_i = \frac{c_2}{\lambda_i}\left[\ln\left(\frac{c_1 \varepsilon_{\max}}{R_i' \lambda_i^5}\right)\right]^{-1}$$

$$\varepsilon_i' = \frac{R_i'}{B_i\left(T'\right)}$$

$$\beta_i = \frac{\varepsilon'_i}{\frac{1}{N}\sum_{i=1}^{N} \varepsilon'_i}$$

$$\varepsilon_{\min} = a + b \cdot MMD^c$$

$$MMD = \max\left(\beta_i\right) - \min\left(\beta_i\right)$$

$$\varepsilon_i = \beta_i \left[\frac{\varepsilon_{\min}}{\min\left(\beta_i\right)}\right]$$

$$T_S = \frac{c_2}{\lambda_i^*}\left[\ln\left(\frac{c_1 \varepsilon_i^*}{R_i^* \lambda_i^{*5}}\right)\right]^{-1}$$

Ouput parameters

*GILLESPIE, A., ROKUGAWA, S., MATSUNAGA, T., COTHERN, J.S., HOOK, S. & KAHLE, A.B. 1998. A temperature and emissivity separation algorithm for Advanced Spaceborne Thermal Emission and Reflection Radiometer (ASTER) images. *IEEE Transactions on Geoscience and Remote Sensing*, 36, 113-1126

Emissivity Methods: TISI

Based on TISI indices using two channels (i,j) and daytime (d) and nightime (n) acquisitions. Accounts for angular dependence.

$$\mathrm{TISI}_{ij} = \frac{B_i(T_{gi}) - R_{at_i\downarrow}}{B_i(T_{gj}) - R_{at_i\downarrow}} = \mathrm{TISIE}_{ij} = \frac{\varepsilon_i}{\varepsilon_j^{n_i/n_j}}$$

$$\mathrm{TISI}_{ij}^{n} = \frac{B_i(T_{gi}^{n}) - R_{at_i\downarrow}^{n}}{B_i(T_{gj}^{n}) - R_{at_i\downarrow}^{n}} \cong \left(\frac{\varepsilon_i}{\varepsilon_j^{n_i/n_j}}\right)^{n} = \mathrm{TISIE}_{ij}^{n}$$

$$TISI_{ij}^{d} = \frac{B_i(T_{gi}^{d}) - (R_{at_i\downarrow}^{d} + R_{sl_i\downarrow})}{B_i(T_{gj}^{d}) - (R_{at_i\downarrow}^{d} + R_{sl_i\downarrow})} = TISIE_{ij}^{d} + \frac{\rho_{bi}(\theta,\varphi,\theta_s,\varphi_s)E_i\cos\theta_s\tau_i(\theta_s,\varphi_s)}{B_i(T_{gj}^{d}) - (R_{at_i\downarrow}^{d} + R_{sl_i\downarrow})}$$

$$\varepsilon_i(\theta) = 1 - \frac{\pi(TISI_{ij}^{d} - TISI_{ij}^{n})(B_i(T_{gj}^{d}) - R_{at_i\downarrow}^{d} - R_{sl_i\downarrow})}{f_i(\theta,\varphi,\theta_s,\varphi_s)E_i\cos\theta_s\tau_i(\theta_s,\varphi_s)} \Longleftrightarrow \varepsilon_j(\theta) = \left(\frac{\varepsilon_i(\theta)}{\mathrm{TISI}_{ij}^{n}}\right)^{n_j/n_i}$$

Emissivity Methods: NDVI Thresholds Method ($NDVI^{THM}$)

LSE from NDVI approaches (sinergy between VNIR & TIR)

Emissivities are obtained from VNIR data, and not from TIR data! This avoids the undetermined problem.

Simplified approach

Emissivity as an average of soil and vegetation emissivities according to the Fractional Vegeetation Cover (FVC).

$$\varepsilon_\lambda = \varepsilon_{s,\lambda}(1-FVC)+\varepsilon_{v,\lambda}FVC$$

$$FVC = \left[\frac{NDVI - NDVIs}{NDVIv - NDVIs}\right]^2$$

NDVI Thresholds Method (Sobrino & Raissouni, 2000)

Pixels are classified into bare pixels, mixed pixels and fully-vegetated pixels. Cavity effect is estimated from a geometric model.

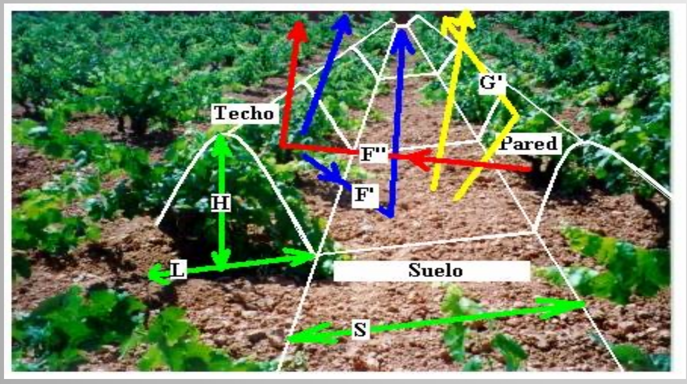

$$\varepsilon_\lambda = \begin{cases} a_\lambda + b_\lambda \rho_{red} & NDVI < NDVIs \\ \varepsilon_{s,\lambda}(1-FVC)+\varepsilon_{v,\lambda}FVC + C_\lambda & NDVIs < NDVI < NDVIv \\ 0.985 + 0.005 & NDVIv \end{cases}$$

$$C_i = (1-\varepsilon_{si})\varepsilon_{vi}F'(1-P_v) \qquad F' = \left(1+\frac{H}{S}\right) - \sqrt{1+\left(\frac{H}{S}\right)^2}$$

Emissivity Methods: Other VIs and Spectral Mixture Analysis (SMA)

LSE from FVC

FVC estimations can be improved by using other retrieval techniques.

Vegetation Indices: NDVI, GVI (VARI)

Spectral Mixture Analysis: requires extraction of endmembers (e.g., land use map, PPI, AMEE)

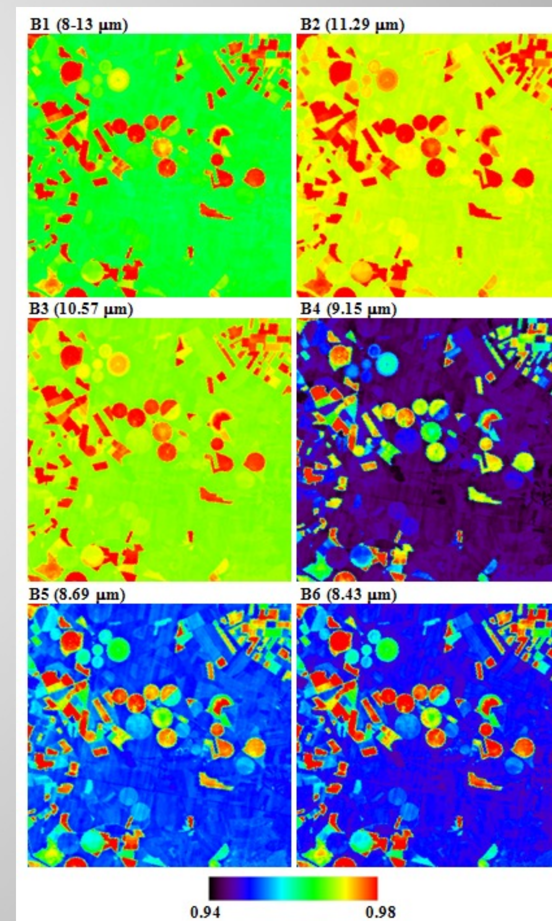

Case study of CHRIS/PROBA *(Sobrino et al., IEEE, 2008; Jiménez-Muñoz et al., Sensors, 2009)*

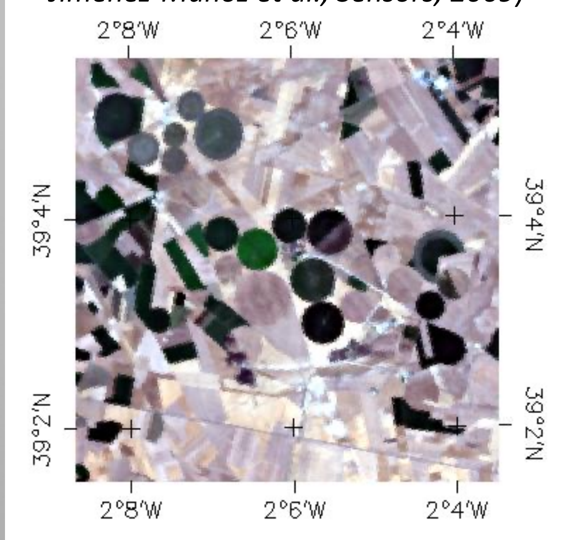

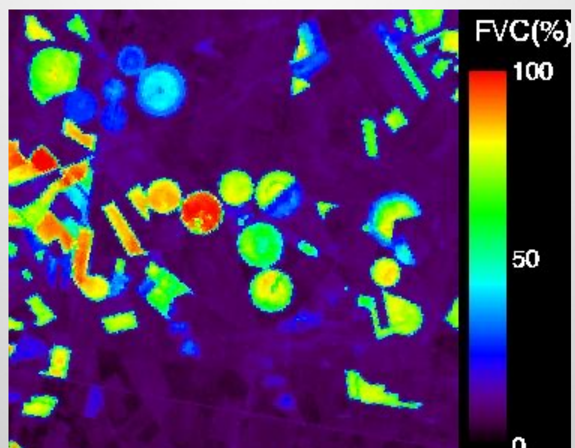

Emissivity Methods: Parametrization based on the gap function

(François et al. 1997)

$$b(\theta) = \exp\left[-\frac{G(\theta)LAI}{\cos\theta}\right]$$

$$\varepsilon_c(\Theta) = 1 - b(\Theta)\, M\, (1 - \varepsilon_g) - \alpha\, [1 - b(\Theta)\, M]\, (1 - \varepsilon_v)$$

Emissivity Methods: BRDF models

(Snyder and Wan, 1998)

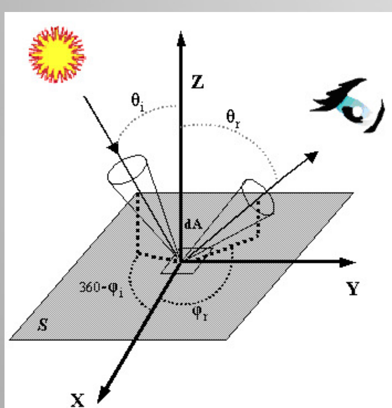

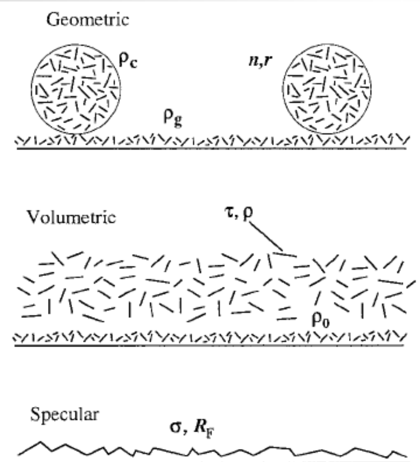

Fig. 2. The scene structures for the geometrical, volumetric, and specular BRDF models. For the geometric case, ρ_c is the Lambertian crown reflectance from the volumetric model, and ρ_g is the Lambertian ground reflectance from the volumetric model or direct measurements. The variables n and r are the number density and radius of the crowns, respectively. For the volumetric model, the randomly oriented facets have a reflectance ρ and a transmission τ. The understory reflectance ρ_0 is from either a volumetric estimate or from direct measurements. The specular model applies the Fresnel reflectance of the surface R_f and a roughness parameter σ.

BRDF obtained from linear combination of kernels

$$f = c_1k_1 + c_2k_2 + c_3$$

Directional emissivity is obtained after hemispherical integration of the BRDF and using Kirchhoff's law (ε=1-ρ)

Example: directional emissivity for different view angles and LAIs
(Sobrino et al., RSE, 2005)

“gap” model

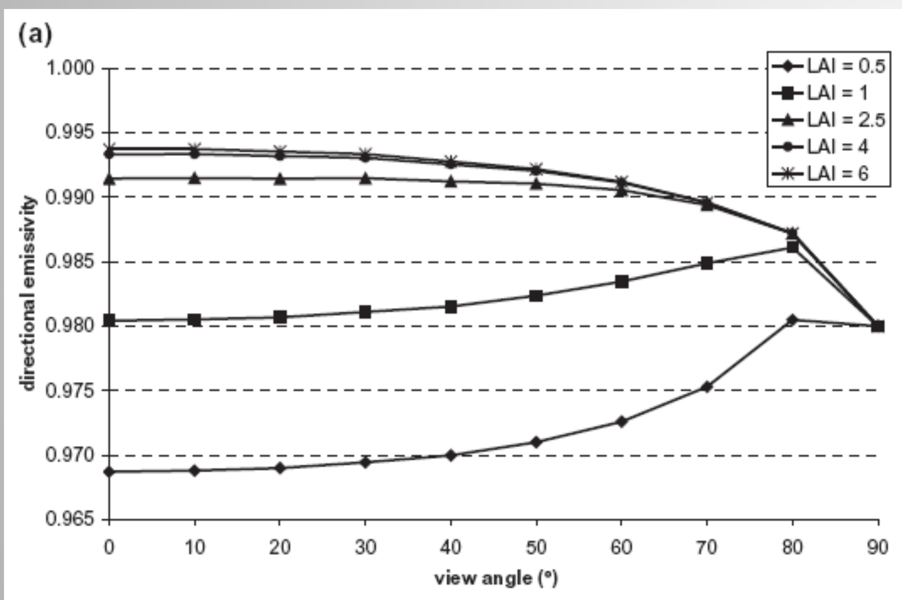

BRDF model